

Structural, Magnetic, and Electrical Study of Polycrystalline $\text{Pr}_{0.55}\text{Sr}_{0.45-x}\text{Na}_x\text{MnO}_3$ ($x = 0.05$ and 0.1)

A. Jerbi¹ · A. Krichene¹ · R. Thaljaoui^{1,2,3} · W. Boujelben¹

Received: 24 June 2015 / Accepted: 12 September 2015 / Published online: 21 September 2015
© Springer Science+Business Media New York 2015

Abstract Structural, magnetic, magnetocaloric, and electrical properties of $\text{Pr}_{0.55}\text{Sr}_{0.45-x}\text{Na}_x\text{MnO}_3$ ($x = 0.05$ and 0.1) have been investigated. Our samples were elaborated using the conventional ceramic method at high temperature. Rietveld refinement of the X-ray diffraction patterns shows that all our compounds are single phase and crystallize in the orthorhombic structure with $Pbnm$ space group. Low field magnetic measurements indicate that all investigated samples exhibit a paramagnetic–ferromagnetic transition with decreasing temperature. This transition takes place at room temperature. A large magnetocaloric effect has been observed in all our compounds. The maximum value of the magnetic entropy change is found to be $3.87 \text{ J K}^{-1} \text{ kg}^{-1}$ for the sample with $x = 0.05$ under $5T$. The values of relative cooling power (RCP) are 246.52 J kg^{-1} for $x = 0.05$ and 262.73 J kg^{-1} for $x = 0.1$, respectively, for an applied magnetic field of $5T$. The electrical resistivity measurements reveal a metal–semiconductor transition with increasing temperature with the presence of a resistivity minimum at

low temperature which is attributed to the electron–electron coulombic interactions.

Keywords Perovskite manganites · Magnetic properties · Magnetocaloric effect · Electrical resistivity

1 Introduction

Magnetic refrigeration technology at room temperature is a possible alternative to conventional gas compression technology due to its easy conception and high energy efficiency [1, 2]. Magnetic refrigeration is based on the magnetocaloric effect (MCE) which consists in the change of a magnetic sample's temperature once we adiabatically apply or remove an external magnetic field. In fact, great works have been performed in order to design a good refrigerator and to look for effective magnetorefrigerants in order to expand the range of temperature and increase efficiency. In the last decades, and after the discovery of the MCE, perovskite manganites having the general formula $\text{Re}_{1-x}\text{Ae}_x\text{MnO}_3$, where Re is a rare earth (La, Pr, Nd...) and Ae is an alkaline earth (Ca, Sr, Ba...) [3–10], have been the aim of intensive research for magnetic refrigeration because of their low cost, easy elaboration procedure, and high chemical stability, compared to gadolinium (Gd) known as the best magnetic refrigerant [11, 12]. Thus, perovskite manganites are suitable candidates in the field of magnetic refrigeration [13–15]. These compounds are characterized by a complex coupling between structural, electrical, and magnetic properties which leads to rich phase diagram [16]. Praseodymium-based compounds are very

✉ A. Krichene
akramkri@hotmail.fr

¹ Laboratoire de Physique des Matériaux, Faculté des Sciences de Sfax, B. P. 1171, 3000 Sfax, Tunisia

² Faculty of Physics, Warsaw University of Technology, Koszykowa 7500-662, Warsaw, Poland

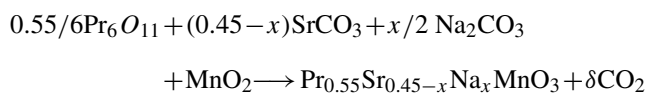
³ Department of Chemistry, University of Warsaw, Al. Zwirki i Wigury 101, 02-089, Warsaw, Poland

interesting since they are characterized by weak double exchange interactions compared to lanthanum-based ones. This fact is attributed to the large lattice distortions. In order to improve the MCE, several works have been done in order to study the effect of doping with monovalent elements [17–19]. The effect of monovalent elements on the magnetic, magnetocaloric, and electrical properties of the compound $\text{Pr}_{0.6}\text{Sr}_{0.4}\text{MnO}_3$ has been intensively studied in the last years [7, 20–25]. In a previous work, we have studied the effect of potassium substitution on the structural, magnetic, magnetocaloric, and electrical properties of $\text{Pr}_{0.55}\text{Sr}_{0.45-x}\text{K}_x\text{MnO}_3$ with $x = 0, 0.05$ and 0.1 , and we have found an important value of relative cooling power (RCP) equal to 247.51 J kg^{-1} for the sample with $x = 0.05$ and a maximum of magnetic entropy change equal to $4.25 \text{ (J kg}^{-1} \text{ K}^{-1})$ for $x = 0.1$; these two values were recorded under an applied magnetic field of $5T$ [3].

Since potassium doping gave interesting results, we have tried in this work to report the effect of the sodium substitution on the structural, magnetic, magnetocaloric, and electrical properties of $\text{Pr}_{0.55}\text{Sr}_{0.45-x}\text{Na}_x\text{MnO}_3$ with $x = 0.05$ and 0.1 in order to compare the effect of sodium with that of potassium. Due to the difference in valency and in the ionic radius of Na^+ and Sr^{2+} , we will obtain a modification in the amount of Mn^{4+} ions, in the average ionic radius at A site $\langle r_A \rangle$ and in the mismatch size of the A cation site σ^2 . The evolution of structural, electrical, and magnetic properties is discussed and analyzed.

2 Experimental Techniques

Polycrystalline samples of $\text{Pr}_{0.55}\text{Sr}_{0.45-x}\text{Na}_x\text{MnO}_3$ ($x = 0.05$ and 0.1) have been prepared using the conventional solid-state reaction method at high temperature by mixing Pr_6O_{11} , SrCO_3 , Na_2CO_3 , and MnO_2 up to 99.9 % high purity in desired proportions according to the following reaction:



The starting materials were heated in air up to $800 \text{ }^\circ\text{C}$ for 24 h, and the obtained powders were then shaped into pellets and fired at $1100 \text{ }^\circ\text{C}$ in air for 24 h with intermediate regrinding and pelletizing. Finally, the obtained pellets were rapidly quenched to room temperature in order to freeze the structure at the annealing temperature. Phase purity and structural parameters were determined by X-ray powder diffraction at room temperature followed by a refinement using the standard Rietveld method [26, 27]. Magnetic

measurements were carried out by a vibrating sample magnetometer in an applied magnetic field up to $5T$. Electrical resistivity was measured by the standard four-probe method.

3 Results and Discussion

3.1 Structural Study

The room temperature X-ray diffraction patterns of our samples are shown in Fig. 1. Refinement results indicate that all our specimens are single phase and are indexed in the orthorhombic system with $Pbnm$ space group, without any detectable impurity. The average crystallite size was evaluated from the width of diffraction peaks by using the Scherrer formula [28] given by

$$C_{\text{XRD}} = K\lambda/\beta \cos \theta \quad (1)$$

where K is the Scherrer constant, λ is the X-ray wavelength, θ is the Bragg angle corresponding to the intense peak, and β is the width at the half maximum of this peak. The average crystallite sizes are listed in Table 1. Using the ionic radii of A, B, and oxygen sites, the tolerance factor t can be evaluated using the following relation:

$$t = \frac{r_A + r_O}{\sqrt{2}(r_B + r_O)} \quad (2)$$

We have gathered in Table 1 the structural analysis results, as well as the average ionic radius at A site $\langle r_A \rangle$, the tolerance factor t , and the cationic mismatch in A site σ^2 for all our samples as well as the parent compound ($x = 0$) [3]. The average ionic radius and the cationic disorder in A site were calculated using Shannon's table for the coordination number 9 [29]. The calculated t values fall in the stable range of the perovskite structure [31]. It is relevant to notice that the lattice parameters verified $c/\sqrt{2} < b < a$ which indicates that the synthesized specimens are characterized by the presence of cooperative Jahn–Teller distortion. In addition, it is obvious from Table 1 that the values of the mismatch σ^2 decrease with increasing sodium content. Thus, the sodium doping leads to the decrease of disorder inside the structure. As we can see from the X-ray diffraction patterns, when Na content increases, this causes a shift in the intense diffraction peak to higher angle values. This result indicates a shrinkage in the unit cell volume as Na content increases. Such evolution can be explained by the cooperative effect of increasing Mn^{4+} content and decreasing the average ionic radius of the A site. In fact, the content of Mn^{4+} increases from 45 % for $x = 0$ to 55 % for $x = 0.1$ and it is known that $r \text{ Mn}^{4+} < r \text{ Mn}^{3+}$ [29],

so it is reasonable to find this drop of the volume. Moreover, the average ionic radius of sodium (1.24 Å) is smaller than that of the strontium one (1.31 Å). In a previous work, the same result was found for $\text{Pr}_{0.6}\text{Sr}_{0.4-x}\text{Na}_x\text{MnO}_3$ [23]; however, it was shown that the substitution with potassium element for $\text{Pr}_{0.55}\text{Sr}_{0.45-x}\text{K}_x\text{MnO}_3$ leads to an increase in the unit cell volume [3]. Besides, if we compare the volume of the $\text{Pr}_{0.55}\text{Sr}_{0.45-x}\text{K}_x\text{MnO}_3$ ($x = 0.05, 0.1$) samples and $\text{Pr}_{0.55}\text{Sr}_{0.45-x}\text{Na}_x\text{MnO}_3$ ($x = 0.05, 0.1$) compounds with a fixed content of Mn^{4+} , the higher values obtained for the potassium-based samples can be explained by the average ionic radius where $r \text{K}^+ > r \text{Na}^+$ [29]. In addition, the

increase of the Mn–O–Mn bond angle for Na-doped samples is overcompensated by the drop in the Mn–O bond length leading to the decrease of the unit cell volume. Using the values of Mn–O–Mn bond angle and Mn–O bond length, we can evaluate the bandwidth W [30] defined as follows [31]:

$$W = \frac{\cos 1/2(\pi - \langle \text{Mn} - \text{O} - \text{Mn} \rangle)}{(d_{\text{Mn} - \text{O}})^{3.5}} \quad (3)$$

We should note that the obtained values of W are 0.0938 and 0.0958 for $x = 0.05$ and 0.1, respectively. One can notice that the $\text{Pr}_{0.55}\text{Sr}_{0.35}\text{Na}_{0.1}\text{MnO}_3$ compound presents

Fig. 1 Rietveld refinement for $\text{Pr}_{0.55}\text{Sr}_{0.45-x}\text{Na}_x\text{MnO}_3$ samples ($x = 0.05$ and 0.1)

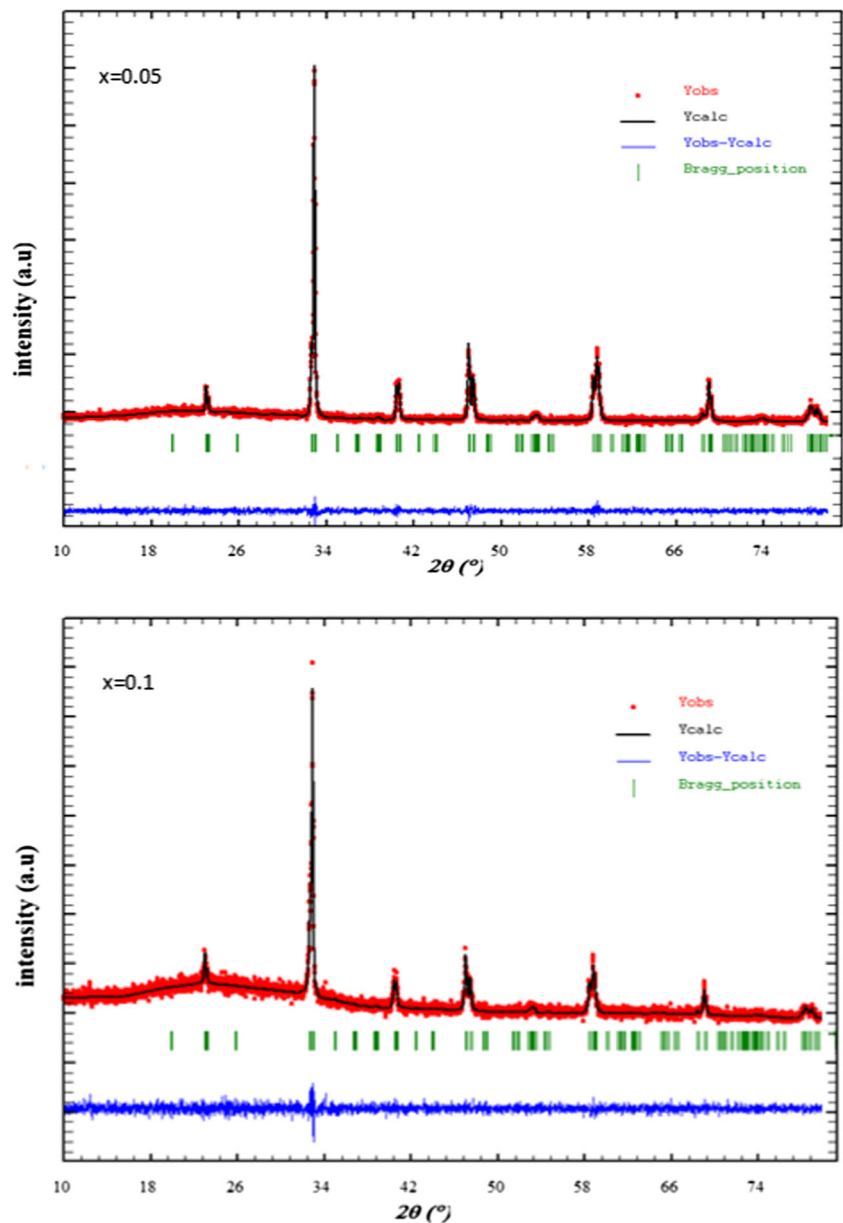


Table 1 The structural results, the average ionic radius, the tolerance factor t , and the cationic disorder in A site for $\text{Pr}_{0.55}\text{Sr}_{0.45-x}\text{Na}_x\text{MnO}_3$ samples ($x = 0, 0.05, \text{ and } 0.1$)

Parameters	$x = 0$ [3]	$x = 0.05$	$x = 0.1$
a (Å)	5.482 (4)	5.485 (3)	5.484 (2)
b (Å)	5.443 (7)	5.442 (3)	5.439 (8)
c (Å)	7.670 (2)	7.663 (2)	7.660 (1)
$c/\sqrt{2}$ (Å)	5.424 (9)	5.418 (7)	5.416 (5)
V (Å) ³	228.901 (9)	228.764 (1)	228.524 (3)
$\langle \text{Mn-O} \rangle$ (Å)	1.962 (5)	1.957 (5)	1.949 (6)
$\langle \text{Mn-O-Mn} \rangle$ (°)	158.869 (3)	160.116 (5)	164.956 (5)
$\langle r_A \rangle$ (Å)	1.237 (9)	1.234 (4)	1.230 (9)
$\sigma^2 \cdot 10^{-3}$ (Å) ²	4.247 (0)	3.975 (7)	3.679(6)
t	0.952 (9)	0.952 (8)	0.953 (1)
Mn^{4+} (%)	45	50	55
C_{XRD} (nm)	33.00	48.75	39.44

the largest Mn–O–Mn bond angle, the lowest Mn–O bond distance, and the most important value of W which leads to lower rotation of the MnO_6 octahedrons. So, we can predict that this sample will have the higher value of Curie temperature.

3.2 Magnetic and Magnetocaloric Study

We have represented in Fig. 2 the evolution of magnetization as a function of temperature in the range 200–400 K under an applied magnetic field of 0.05 T for the samples $\text{Pr}_{0.55}\text{Sr}_{0.45-x}\text{Na}_x\text{MnO}_3$ with $0 \leq x \leq 0.1$. It seems that all our compounds present a transition from paramagnetic to ferromagnetic state with decreasing temperature. The Curie temperature values were determined using the tangent method. They present a slight decrease with increasing sodium content from 304 K for the parent sample [3] to 300 K for $x = 0.05$ and 290 K for $x = 0.1$. Similar results were obtained with the sodium substitution on

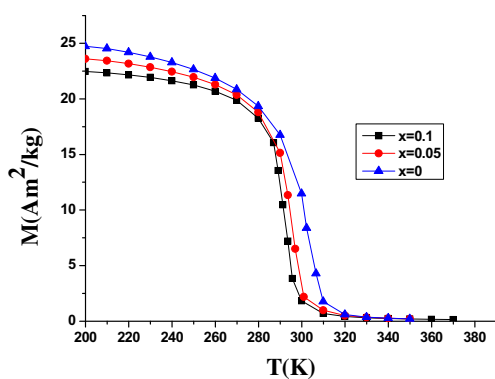


Fig. 2 Temperature dependence of magnetization for $\text{Pr}_{0.55}\text{Sr}_{0.45-x}\text{Na}_x\text{MnO}_3$ samples ($x = 0, 0.05, \text{ and } 0.1$)

$\text{Pr}_{0.6}\text{Sr}_{0.4}\text{MnO}_3$ [23] and with the potassium substitution on $\text{Pr}_{0.55}\text{Sr}_{0.45}\text{MnO}_3$ [3]. It is important to note that the substitution did not strongly affect the Curie temperature T_C value which remains close to room temperature for all samples; such properties are required to get a magnetic refrigerant which is active at room temperature. Through the structural study, it was expected that the sample with $x = 0.1$ will present the highest value of the T_C since it presents the lowest value of the Mn–O distance and mismatch σ^2 and the highest value of Mn–O–Mn bond angle and W which enhances ferromagnetic double exchange mechanism, but it is not the case. Generally, the evolution of the Curie temperature can be governed by the ionic radius of the A site $\langle r_A \rangle$, the amount of the Mn^{4+} , and the mismatch effect. In fact, the increase of the average of Mn^{4+} from 45 to 55 % causes a weakness of ferromagnetism which induces the decrease of the Curie temperature T_C . In addition, the T_C reduction is affected by the slight decrease of the ionic radius values from 1.24 Å for $x = 0$ to 1.23 Å for $x = 0.1$. The disorder cannot explain the T_C evolution since we have a decrease in the values of σ^2 from $4.247 \cdot 10^{-3} \text{ Å}^2$ for $x = 0$ to $3.679 \cdot 10^{-3} \text{ Å}^2$ for $x = 0.1$. So, even the structure

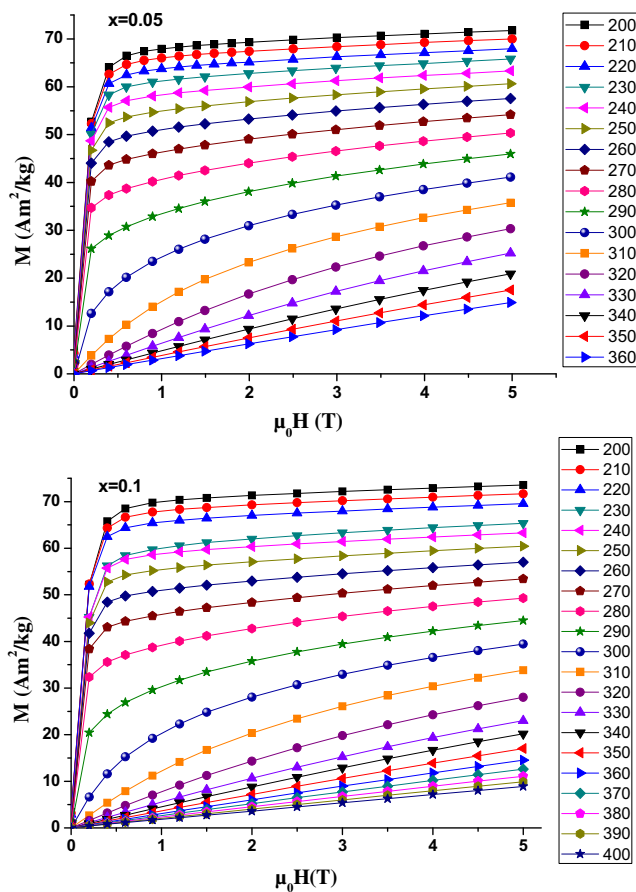


Fig. 3 Magnetic applied field dependence of magnetization at several temperatures for $\text{Pr}_{0.55}\text{Sr}_{0.45-x}\text{Na}_x\text{MnO}_3$ samples ($x = 0.05 \text{ and } 0.1$)

becomes more ordered; the decrease of T_C is attributed to the cooperative effect of both $\langle r_A \rangle$ and Mn^{4+} amount.

The isothermal magnetization obtained under magnetic applied field up to 5T in temperature range 200–400 K for our Na-substituted samples is shown in Fig. 3. It is clear that the magnetization increases sharply under 0.5T for low temperature values and then starts to saturate above 1T which confirms the low-temperature ferromagnetic state observed from the $M(T)$ curves. We can notice that $M(H)$ curves are not linear for our substituted compounds above T_C which can be explained by the presence of some ferromagnetic ordering above T_C . The same behavior was observed in $Pr_{0.55}Sr_{0.45-x}K_xMnO_3$ ($x = 0.05, x = 0.1$) [3]. In order to confirm the existence of such interactions, we have represented in Fig. 4 the temperature dependence of the inverse of paramagnetic susceptibility for our investigated samples. We can notice that the linear dependence of χ^{-1} as a function of temperature is in a perfect agreement with the Curie–Weiss law given by

$$\chi = \frac{C_p}{T - \theta_p} \tag{4}$$

where C_p is the Curie constant and θ_p is the Weiss temperature. The values of θ_p are found to be 305 K for $x = 0.05$ and 295 K for $x = 0.1$, respectively. It is obvious that the paramagnetic Weiss temperature decreases with increasing sodium content. This tendency reflects a reduction in ferromagnetic double exchange interactions when Mn^{4+} content changes from 45 to 55 %. Indeed, the observed difference between θ_p and T_C indicates the presence of a short-range magnetic ordering in the paramagnetic phase near T_C and confirms the results obtained from $M(H)$ curves. From the

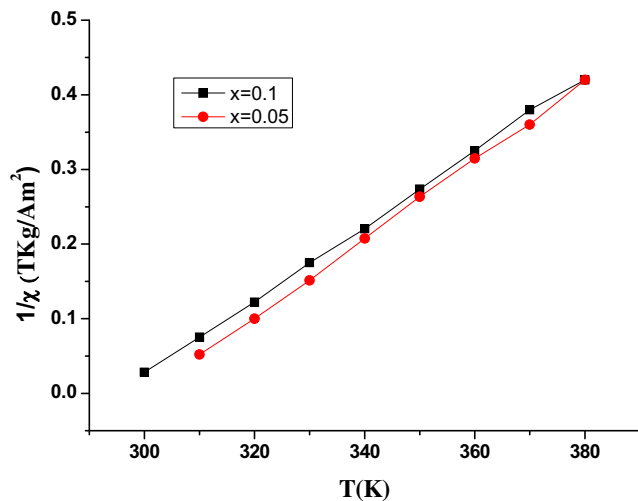


Fig. 4 Temperature dependence of the inverse of paramagnetic susceptibility for $Pr_{0.55}Sr_{0.45-x}Na_xMnO_3$ samples ($x = 0.05$ and 0.1)

fitting of the high-temperature linear part of $\chi^{-1}(T)$, we can deduce the Curie constant C_p which is given by

$$C_p = \mu_0 \mu_{\text{eff}}^2 / 3k_B \tag{5}$$

where $\mu_0 = 4\pi \cdot 10^{-7} \text{ H m}^{-1}$ is the permeability, $\mu_B = 9.27 \cdot 10^{-24} \text{ J T}^{-1}$ is the Bohr magnetron, and $k_B = 1.38 \cdot 10^{-23} \text{ J K}^{-1}$ is the Boltzmann constant. The constant C_p is used to estimate the experimental effective paramagnetic moment μ_{eff} . For our samples, we found that μ_{eff} values are $5.7\mu_B$ and $5.83\mu_B$ for $x = 0.05$ and $x = 0.1$, respectively. The theoretically predicted values for $Pr_{0.55}Sr_{0.4}Na_{0.05}MnO_3$ and $Pr_{0.55}Sr_{0.35}Na_{0.1}MnO_3$ are $5.15\mu_B$ and $5.11\mu_B$, respectively. It is relevant that the experimental values are more important than the theoretical ones suggesting strong ferromagnetic correlation in the paramagnetic state above T_C , which also confirms the observed behavior in the $M(H)$ curves. In order to clarify

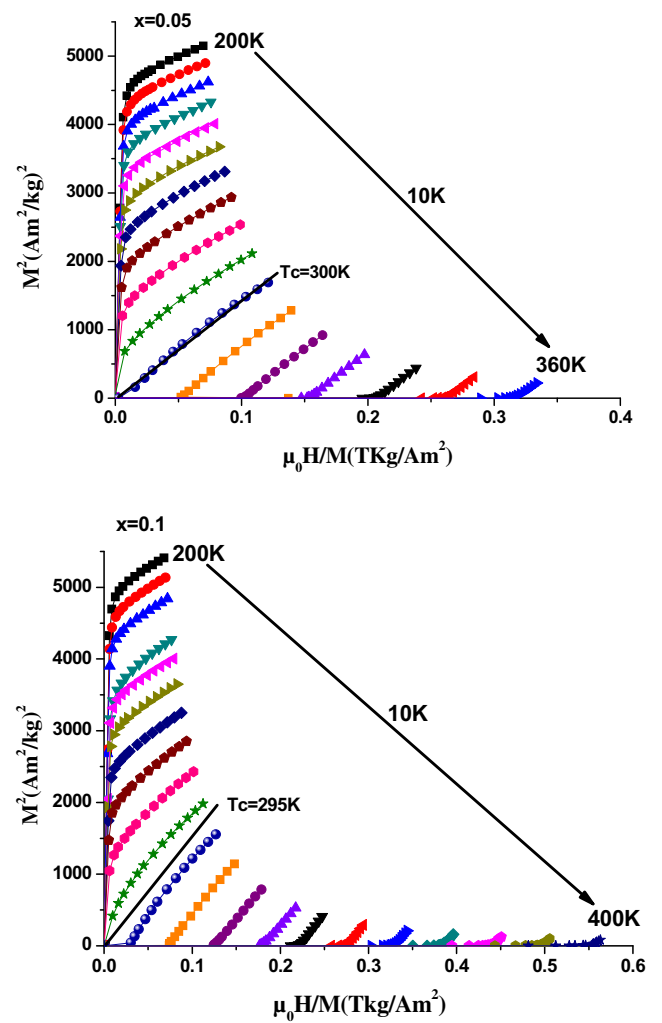
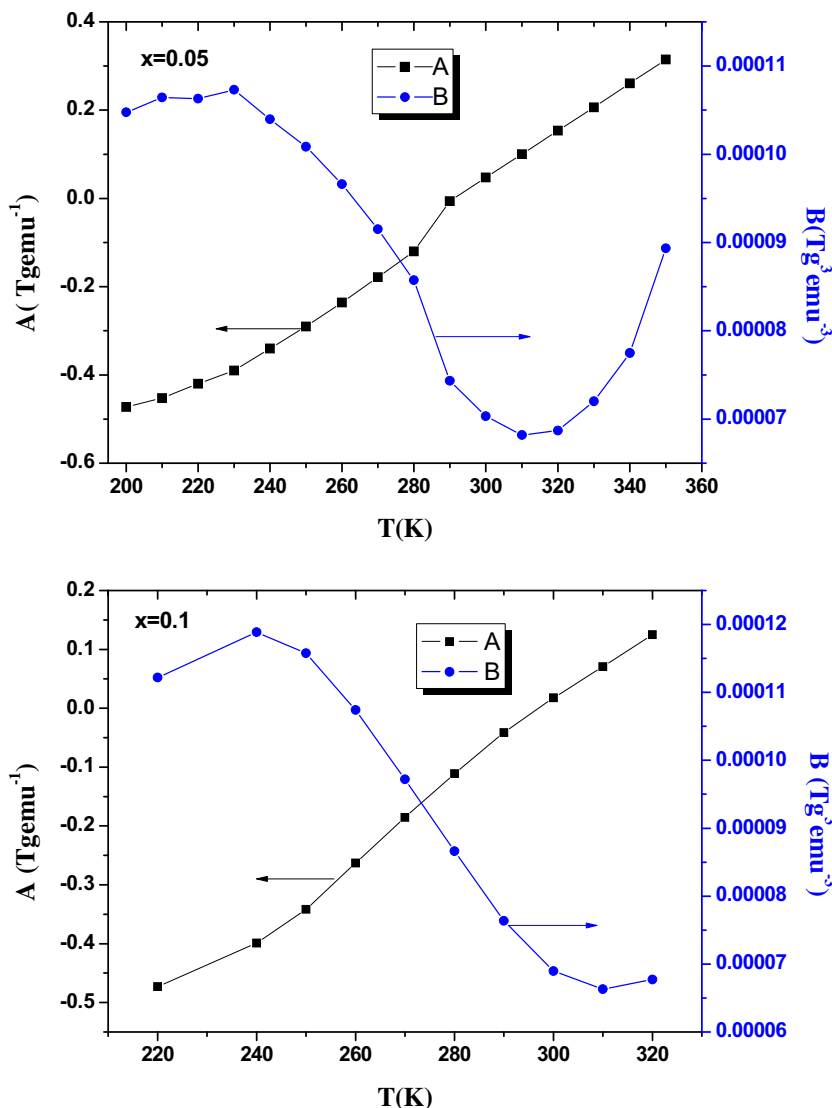


Fig. 5 Arrott plots for $Pr_{0.55}Sr_{0.45-x}Na_xMnO_3$ samples ($x = 0.05$ and 0.1)

Fig. 6 *A* and *B* parameters versus temperature for $\text{Pr}_{0.55}\text{Sr}_{0.45-x}\text{Na}_x\text{MnO}_3$ samples ($x = 0.05$ and 0.1)



the nature of the phase transition and to confirm the values of the Curie temperature, the Arrott plots for our doped samples are represented in Fig. 5. These plots represent the evolution of M^2 as a function of $\mu_0 H/M$. According to classical thermodynamic relation, we can write:

$$\mu_0 H/M = A(T) + B(T) M^2 \tag{6}$$

The *A* and *B* parameters corresponding to the intercept and the slope of linear part of plots, respectively, are determined by fitting. The temperature dependence of *A* and *B* parameters are represented in Fig. 6. In fact, the T_C value is revealed by a sign change of the *A* parameter. The obtained values are 298 and 290 K for $x = 0.05$ and $x = 0.1$, respectively, which agrees with the values obtained from the $M(T)$ curves. Besides, the *B* parameter is positive in the studied temperature range which indicates that the paramagnetic–ferromagnetic transition is a second ordered one [33, 34].

In order to confirm the effectiveness of our samples as good candidates in the magnetic refrigeration domain, temperature dependence of magnetic entropy change under several values of magnetic field up to 5T is reported in Fig. 7. The magnetic entropy change ($-\Delta S_M$) can be calculated according to the classical thermodynamic theory based on Maxwell’s relations using the following equation:

$$\Delta S_M(T, H) = \sum_i \frac{M_{i+1}(T_{i+1}, H) - M_i(T_i, H)}{T_{i+1} - T_i} \Delta H \tag{7}$$

where M_i and M_{i+1} are the experimental values of magnetization measured at temperatures T_i and T_{i+1} , respectively, under magnetic applied field H_i . All our doped samples present an important MCE effect in vicinity of room temperature, and the magnitude of ΔS_M increases with increasing applied magnetic field. Compared to the parent sample where $\Delta S_M = 3.326 \text{ J kg}^{-1} \text{ K}^{-1}$ [3], the ($-\Delta S_M$) values for our substituted specimens increase to $3.87 \text{ J kg}^{-1} \text{ K}^{-1}$ for

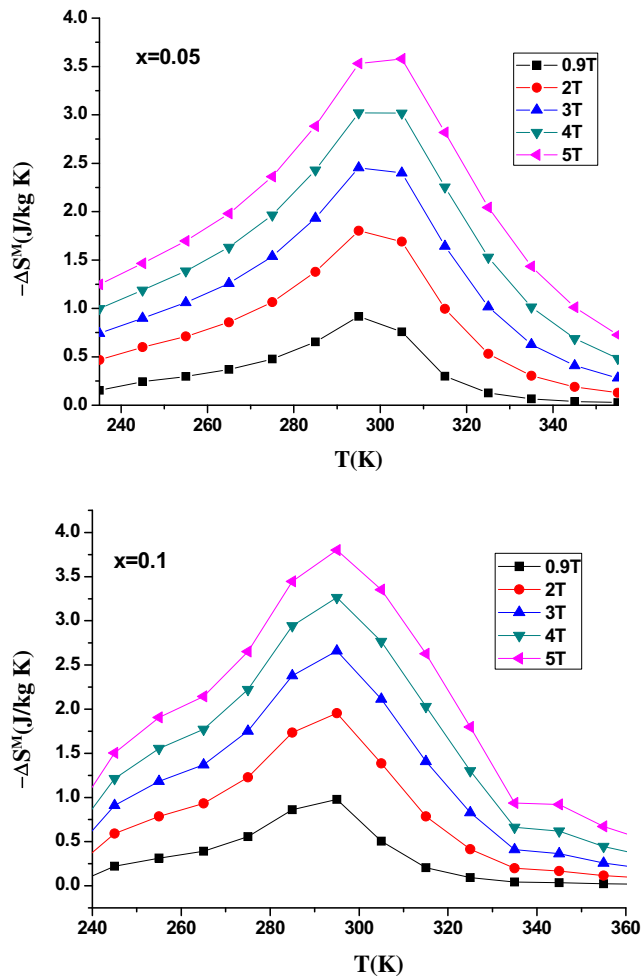


Fig. 7 Temperature dependence of magnetic entropy change at several values of magnetic applied field for $\text{Pr}_{0.55}\text{Sr}_{0.45-x}\text{Na}_x\text{MnO}_3$ samples ($x = 0.05$ and 0.1)

$x = 0.05$ and $3.8 \text{ J kg}^{-1} \text{ K}^{-1}$ for $x = 0.1$ under a magnetic applied field of $5T$. For a magnetic applied field of $2T$, we have found a value of the ΔS_M equal to $1.95 \text{ J kg}^{-1} \text{ K}^{-1}$ for $x = 0.1$ which is more important than $1.32 \text{ J kg}^{-1} \text{ K}^{-1}$ obtained for $\text{Pr}_{0.6}\text{Sr}_{0.3}\text{Na}_{0.1}\text{MnO}_3$ [8]. The increase of the maximum of the magnetic entropy change can be explained by the decrease of the mismatch effect [32]. It is important to determine not only the magnitude of the magnetic entropy change but also the width of the $\Delta S_M(T)$ peak. So, we should calculate the relative cooling power (RCP) which can be evaluated using the following relation:

$$RCP(S) = -\Delta S_M(T, H) \times \delta T_{FWHM} \tag{8}$$

where δT_{FWHM} is the full width at the half maximum of $\Delta S_M(T)$ [30]. For our samples, the values of RCP are 246.52 J kg^{-1} for $x = 0.05$ and 262.73 J kg^{-1} for $x = 0.1$, respectively, for an applied magnetic field of $5T$. Compared to the samples doped with the potassium element [3], it is

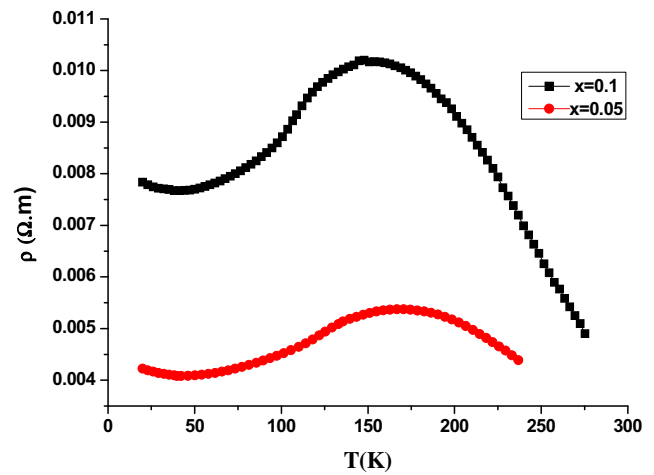


Fig. 8 The temperature dependence of resistivity for $\text{Pr}_{0.55}\text{Sr}_{0.45-x}\text{Na}_x\text{MnO}_3$ samples ($x = 0.05$ and 0.1)

clear that the sodium-doped samples present more important values of RCP. Thus, our samples can be considered as well candidates in the magnetic refrigeration field

3.3 Electrical Properties

In order to investigate the effect of the sodium element on the electrical properties of our samples, we have reported resistivity measurements versus temperature in the temperature range $20\text{--}280 \text{ K}$ for all our elaborated compounds under earth’s magnetic field. Our measurements are represented in Fig. 8. It is clear that our doped samples possess the same electrical behavior. When temperature decreases, the specimens exhibit a transition from semiconducting to metallic state at the transition temperature T_ρ with the presence of a resistivity minimum near 42 K . We found that the electrical temperature transition is equal to 169.2 and 153.7 K

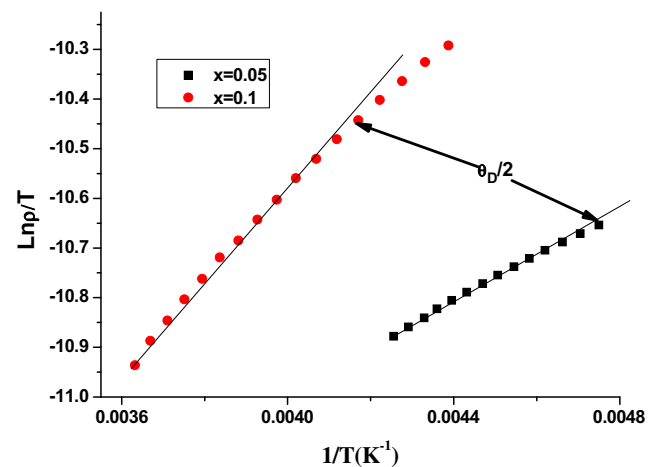


Fig. 9 The evolution of $\text{Ln}(\rho/T)$ as a function of the inverse of temperature for $\text{Pr}_{0.55}\text{Sr}_{0.45-x}\text{Na}_x\text{MnO}_3$ samples ($x = 0.05$ and 0.1)

for $x = 0.05$ and $x = 0.1$, respectively. The obtained values are still lower than $T_\rho = 194.5$ K observed for the undoped manganite $\text{Pr}_{0.55}\text{Sr}_{0.45}\text{MnO}_3$ [3]. Such difference can be explained by the amount of Mn^{4+} ions. In fact, increasing Na content leads to the increase of Mn^{4+} amount which promotes super exchange mechanism in favor of double exchange one and shifts the transition temperature to lower values. Besides, it is worthy to notice that T_ρ values are remarkably lower than the Curie temperature; the same behavior has been also reported for other doped manganites [3]. This difference can be related to the small crystallite sizes which perturb the surface layer. In fact, the small crystallite size leads to the enhancement of electron scattering at grain boundaries and leads to poor connectivity between grains [35]. The electrical resistivity values did not exceed $11 \text{ m}\Omega \text{ m}$ for all our samples which confirms that the ground state is ferromagnetic. The resistivity reduction reveals only a partial melting of charge ordered phase into the ferromagnetic metallic phase. The same behavior was observed for $\text{Pr}_{0.55}\text{Na}_{0.05}\text{Sr}_{0.4}\text{MnO}_3$ [24]. The electrical transport mechanism in manganites can be governed by several models.

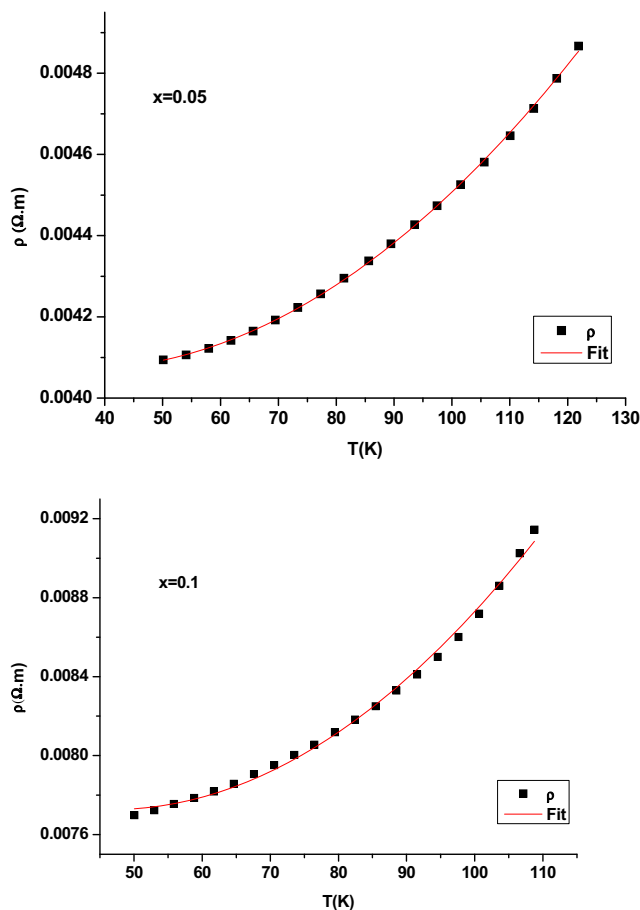


Fig. 10 The evolution of the resistivity as a function of the temperature below T_ρ for $\text{Pr}_{0.55}\text{Sr}_{0.45-x}\text{Na}_x\text{MnO}_3$ samples ($x = 0.05$ and 0.1). The red line presents the fitting according to (11)

The temperature dependence of electrical resistivity in semi-conducting phase above T_ρ for all our samples was analyzed with the small polaron hopping (SPH) model above $\theta_D/2$ (where θ_D is the Debye temperature) given by the following equation:

$$\rho(T) = \rho_0 T \exp(E_{\text{hopp}}/kT) \quad (9)$$

where ρ_0 is a constant, E_{hopp} is the hopping energy, and k is Boltzmann constant. The linear dependence of $\text{Ln}(\rho/T)$ as a function of T^{-1} for our samples as presented in Fig. 9 confirms the validity of this model. The values of θ_D found from the deviation of the linearity in the low temperature are 421 and 474 K for $x = 0.05$ and $x = 0.1$, respectively. For $x = 0.1$, we have found the maximum value of hopping energy which can be explained by the reduction of double exchange mechanism which limits e_g electron hopping. Using the values of θ_D , we can evaluate the frequency of the longitudinal optical phonon ν_{ph} by the following equation:

$$h\nu_{ph} = k\theta_D \quad (10)$$

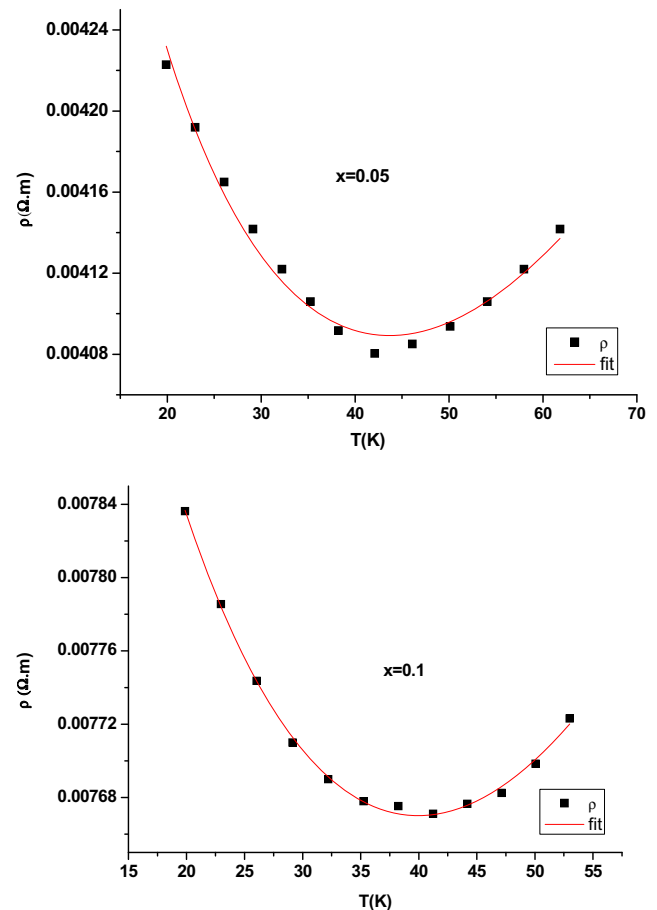


Fig. 11 The evolution of the resistivity as a function of the temperature for $\text{Pr}_{0.55}\text{Sr}_{0.45-x}\text{Na}_x\text{MnO}_3$ ($x = 0.05$ and 0.1). The red line presents the fitting according to (13)

Table 2 Best fit values of resistivity data

Samples	Pr _{0.55} Sr _{0.4} Na _{0.05} MnO ₃	Pr _{0.55} Sr _{0.35} Na _{0.1} MnO ₃
E_{hopp} (meV)	39.67	74.63
A ($10^{-7}\Omega \text{ mK}^{-2}$)	1.053	3.517
$\rho(0)$ (m Ω m)	4.2	8.5
α ($\Omega \text{ cm}$)	0.548	0.917
β ($10^{-2}\Omega \text{ cm K}^{-0.5}$)	4.376	3.694
γ ($10^{-4}\Omega \text{ cm K}^{-n}$)	39.574	4.888
n	0.9628	1.3947
a ($\Omega \text{ cm}$) ⁻¹	1.8248	1.0905
b ($\Omega \text{ cm K}^{0.5}$) ⁻¹	0.1457	0.04392
ν_{ph} (10^{12} Hz)	8.77	9.88

where h is the Planck constant. At low temperature and below T_{ρ} , we have found that the thermal variations of the resistivity for our samples can be described by the relation:

$$\rho(T) = \rho(0) + AT^2 \tag{11}$$

where $\rho(0)$ is a temperature-independent low temperature resistivity due to the scattering by impurities, grain boundaries, and domain walls [36] and the A term is ascribed to the electron–electron or single magnon scattering [37, 38]. Figure 10 confirms the validity of this relation at low temperature ($T < T_{\rho}$). These results indicate that the electron–electron scattering process plays an important role in our compounds [39, 40]. Moreover, we have previously indicated that our specimens present a resistivity minimum in vicinity of 42 K. Various models have been proposed in order to explain this behavior at low temperature [41–45]. Such behavior was observed for the first time in magnetically diluted alloys by Kondo [46]. In our case, the ground state is ferromagnetic which implies that Kondo effect cannot be responsible for the presence of low temperature resistivity minimum. For our compound, we have found that the fitting results obey the following equation:

$$\rho(T) = \left\{ \frac{1}{a + bT^{1/2}} \right\} + \gamma T^n \tag{12}$$

Equation (12) can be written as follows:

$$\rho = \alpha - \beta\sqrt{T} + \gamma T^n \tag{13}$$

In this equation, the first term $\alpha = 1/a$ is the residual resistivity, the second term $\beta\sqrt{T}$ (with $\beta = b/a^2$) is ascribed to the electron–electron coulombic interaction enhanced by decreasing the temperature, and the third term γT^n gathers the inelastic scattering processes including the electron–phonon interaction, the electron–magnon interaction.... We have represented in Fig. 11 the temperature dependence of resistivity for $T < 60$ K as well as experimental data fitting using the relation (13). One can notice from Fig. 11 a strong correlation between experimental and theoretical

data which confirms the validity of the used model. The best values of fitting parameters obtained from resistivity data, the frequency ν_{ph} , a and b parameters for our samples are summarized in Table 2. It is obvious that the sample with $x = 0.05$ presents the highest values of β and γ which indicates that elastic and inelastic scattering mechanisms are reduced by sodium doping.

4 Conclusion

We have investigated structural, magnetic, and electrical properties of Pr_{0.55}Sr_{0.45-x}Na_xMnO₃ samples with $x = 0.05$ and 0.1 . Structural analysis revealed that all our samples crystallize in the orthorhombic structure with $Pbnm$ space group. Magnetic measurements showed a paramagnetic–ferromagnetic transition with decreasing temperature which takes place around room temperature for all our samples. Sodium-based samples were characterized by an important MCE near room temperature which gives the possibility to use them as magnetic refrigerants. Electrical resistivity measurements revealed the presence of a metal–semiconductor transition with increasing temperature. The presence of resistivity minimum around 42 K was attributed to the electron–electron coulombic interactions.

Acknowledgments This work was supported by the Tunisian Ministry of Higher Education and Scientific Research.

References

- Gschneidner, K.A.Jr., Pecharsky, V.K., Tsokol, A.O.: Recent developments in magnetocaloric materials. Rep. Prog. Phys. **68**, 1479 (2005)
- Zhang, X.Y., Chen, Y., Li, Z.Y.: A potential oxide for magnetic refrigeration application: CrO₂ particles. J. Phys.: Condens. Matter **18**, L559 (2006)
- Jerbi, A., Thaljaoui, R., Krichene, A., Boujelben, W.: Structural, magnetic and magnetocaloric study of polycrystalline Pr_{0.55}Sr_{0.45-x}K_xMnO₃ ($x=0, 0.05$ and 0.1). Physica B **442**, 21 (2014)
- Mehri, A., Cheikh-Rouhou Koubaa, W., Koubaa, M., Cheikh-Rouhou, A.: Magnetic and magnetocaloric properties of monovalent substituted La_{0.5}Ca_{0.45}A_{0.05}MnO₃ (A=Na, Ag, K) perovskite manganites. Mater. Sci. Eng. **28**, 012049 (2012)
- Regaieg, Y., Koubaa, M., Cheikhrouhou Koubaa, W., Cheikhrouhou, A., Sicard, L., Ammar-Merah, S., Herbst, F.: Structure and magnetocaloric properties of La_{0.8}Ag_{0.2-x}K_xMnO₃ perovskite manganites. Mater. Chem. Phys. **132**, 839 (2012)
- Ayadi, F., Saadaoui, F., Cheikhrouhou-Koubaa, W., Koubaa, M., Cheikhrouhou, A., Sicard, L., Ammar, S.: Effect of monovalent doping on the physical properties of La_{0.7}Sr_{0.3}MnO₃ compound synthesized using sol-gel technique. Mater. Sci. Eng. **28**, 012054 (2012)
- Thaljaoui, R., Boujelben, W., Pekała, M., Pocięcha, D., Szydłowska, J., Cheikhrouhou, A.: Room temperature magnetocaloric and magneto-transport properties of monovalent doped

- $\text{Pr}_{0.6}\text{Sr}_{0.35}\text{Na}_{0.05}\text{MnO}_3$ manganite. *J. Alloys Compd.* **530**, 138 (2012)
8. Koubaa, M., Cheikh-Rouhou Koubaa, W., Cheikhrouhou, A.: Magnetocaloric effect and magnetic properties of $\text{La}_{0.75}\text{Ba}_{0.1}\text{M}_{0.15}\text{MnO}_3$ (M=Na, Ag and K) perovskite manganites. *J. Alloys Compd.* **479**, 65 (2009)
 9. Koubaa, M., Regaieg, Y., Cheikhrouhou Koubaa, W., Cheikhrouhou, A., Ammar-Merah, S., Herbst, F.: Magnetic and magnetocaloric properties of lanthanum manganites with monovalent elements doping at A-site. *J. Magn. Magn. Mat.* **323**, 252 (2011)
 10. Cheikh-Rouhou Koubaa, W., Koubaa, M., Cheikhrouhou, A.: Effect of monovalent doping on the structural, magnetic and magnetocaloric properties in $\text{La}_{0.7}\text{M}_{0.2}\text{M}'_{0.1}\text{MnO}_3$ manganese oxides (M=Sr, Ba and M'=Na, Ag, K). *Phys. Procedia* **2**, 989 (2009)
 11. Pecharsky, V.K., Gschneidner, K.A.: Effect of alloying on the giant magnetocaloric effect of $\text{Gd}_5(\text{Si}_2\text{Ge}_2)$. *J. Magn. Magn. Mat.* **167**, 1179 (1997)
 12. Zimm, C., Sternberg, A., Pecharsky, V., Gschneidner, K.Jr., Osborne, M., Anderson, I.: Description and performance of a near-room temperature magnetic refrigerator. *Adv. Cryog. Eng.* **43**, 1759 (1998)
 13. Guo, Z.B., Du, Y.W., Zhu, J.S., Huang, H., Ding, W.P., Feng, D.: Large magnetic entropy change in perovskite-type manganese oxides. *Phys. Rev. Lett.* **78**, 1142 (1997)
 14. Phan, M.H., Yu, S.C.: Review of the magnetocaloric effect in manganite materials. *J. Magn. Magn. Mater.* **308**, 325 (2007)
 15. Gencer, H., Atalay, S., Adiguzel, H.I., Kolat, V.S.: Magnetocaloric effect in the $\text{La}_{0.62}\text{Bi}_{0.05}\text{Ca}_{0.33}\text{MnO}_3$ compound. *Physica B* **357**, 326 (2005)
 16. Martin, C., Maignan, A., Hervieu, H., Raveau, B.: Magnetic phase diagrams of $\text{L}_{1-x}\text{A}_x\text{MnO}_3$ manganites (L=Pr, Sm; A=Ca, Sr). *Phys. Rev. B* **60**, 12191 (1999)
 17. Das, S., Dey, T.K.: Structural and magnetocaloric properties of $\text{La}_{1-y}\text{Na}_y\text{MnO}_3$ compounds prepared by microwave processing. *J. Phys. D: Appl. Phys.* **40**, 1855 (2007)
 18. Gamzatov, A.G., Batdalov, A.B., Kamilov, I.K.: Correlation of electrical and thermalphysical properties of $\text{La}_{0.85}\text{Ag}_{0.15}\text{MnO}_3$ manganite. *Physica B* **406**, 2231 (2011)
 19. Aliev, A.M., Gamzatov, A.G., Batdalov, A.B., Mankevich, A.S., Korsakov, I.E.: Structure and magnetocaloric properties of $\text{La}_{1-x}\text{K}_x\text{MnO}_3$ manganites. *Physica B* **406**, 885 (2011)
 20. Thaljaoui, R., Pekała, K., Pekała, M., Boujelben, W., Szydłowska, J., Fagnard, J.-F., Vanderbenden, P., Cheikhrouhou, A.: Magnetic susceptibility and electron magnetic resonance study of monovalent potassium doped manganites $\text{Pr}_{0.6}\text{Sr}_{0.4-x}\text{K}_x\text{MnO}_3$. *J. Alloys Compd.* **580**, 137 (2013)
 21. Thaljaoui, R., Boujelben, W., Pekała, M., Szydłowska, J., Cheikhrouhou, A.: Electron magnetic resonance study of monovalent Na doping in $\text{Pr}_{0.6}\text{Sr}_{0.4-x}\text{Na}_x\text{MnO}_3$ manganites. *J. Alloys Compd.* **526**, 98 (2012)
 22. Thaljaoui, R., Boujelben, W., Pekała, M., Pekała, K., Cheikhrouhou, A.: Structural and electrical properties of monovalent doped manganites $\text{Pr}_{0.6}\text{Sr}_{0.4-x}\text{K}_x\text{MnO}_3$ ($x=0, 0.05$ and 0.1). *J. Supercond. Nov. Magn.* **26**, 1625 (2013)
 23. Thaljaoui, R., Boujelben, W., Pekała, K., Pekała, M., Cheikhrouhou-Koubaa, W., Cheikhrouhou, A.: Magnetocaloric study of monovalent-doped manganites $\text{Pr}_{0.6}\text{Sr}_{0.4-x}\text{Na}_x\text{MnO}_3$ ($x=-0.2$). *J. Mater. Sci.* **48**, 3894 (2013)
 24. Thaljaoui, R., Boujelben, W., Pekała, M., Pekała, K., Mucha, J., Cheikhrouhou, A.: Structural, magnetic and transport study of monovalent Na-doped manganite $\text{Pr}_{0.55}\text{Na}_{0.05}\text{Sr}_{0.4}\text{MnO}_3$. *J. Alloys Compd.* **558**, 236 (2013)
 25. Thaljaoui, R., Boujelben, W., Pekała, M., Pekała, K., Fagnard, J.-F., Vanderbenden, P., Donton, M., Cheikhrouhou, A.: Magnetocaloric effect of monovalent K doped manganites $\text{Pr}_{0.6}\text{Sr}_{0.4-x}\text{K}_x\text{MnO}_3$ ($x=0$ to 0.2). *J. Magn. Magn. Mater.* **352**, 6 (2014)
 26. Rietveld, H.M.: A profile refinement method for nuclear and magnetic structures. *J. App. Cryst.* **2**, 65 (1969)
 27. Roisnel, T., Rodriguez-Carvajal, J.: Computer program FULLPROF, LLB-LCSIM (2003)
 28. Taylor, A.: X-ray Metallography. Wiley, New York (1961)
 29. Shannon, R.D.: Revised effective ionic radii and systematic studies of interatomic distances in Halides and Chalcogenides. *Acta crystallogr.* **A32**, 751–767 (1976)
 30. Kittel, C. Introduction to solid state physics, 6th edn., pp. 404–406. Wiley, New York
 31. Medarde, M., Mesot, J., Lacorre, P., Rosenkranz, S., Fisher, P., Gobrecht, K.: High-pressure neutron-diffraction study of the metallization process in PrNiO_3 . *Phys. Rev. B* **52**, 9248 (1995)
 32. Koubaa, M., Cheikh-Rouhou Koubaa, W., Cheikhrouhou, A.: Magnetocaloric effect in polycrystalline $\text{La}_{0.65}\text{Ba}_{0.3}\text{M}_{0.05}\text{MnO}_3$ (M=Na, Ag, K) manganites. *J. Magn. Magn. Mat.* **321**, 3578 (2009)
 33. Banerjee, S.K.: On a generalised approach to first and second order magnetic transitions. *Phys. Lett.* **12**, 16–17 (1964)
 34. Landau, L.D., Lifshitz, E.M. Statistical physics, 3rd edn. Pergamon, Oxford (1980)
 35. de Andres, A., Garcia-Hernandez, M., Martinez, J.L., Prieto, C.: Low-temperature magnetoresistance in polycrystalline manganites: connectivity versus grain size. *Appl. Phys. Lett.* **74**, 3884 (1999)
 36. Mott, N.F.: Metal–insulator transition, p. 51. Taylor and Francis (1990)
 37. Ibrahim, N., Yahya, A.K., Rajput, S.S., Keshri, S., Talari, M.K.: Double metal–insulator peaks and effect of Sm^{3+} substitution on magnetic and transport properties of hole-doped $\text{La}_{0.85}\text{Ag}_{0.15}\text{MnO}_3$. *J. Magn. Magn. Mater.* **323**, 2179 (2011)
 38. Padmavathi, K., Venkataiah, G., Venugopal Reddy, P.: Electrical behavior of some rare-earth-doped $\text{Nd}_{0.33}\text{Ln}_{0.34}\text{Sr}_{0.33}\text{MnO}_3$ manganites. *J. Magn. Magn. Mater.* **309**, 237 (2007)
 39. Viret, M., Ranno, L., Coey, J.M.D.: Magnetic localization in mixed-valence manganite. *Phys. Rev. B* **55**, 8067 (1997)
 40. Callaway, J.: Model for lattice thermal conductivity at low temperatures. *Phys. Rev.* **113**, 1046 (1959)
 41. Krichene, A., Solanki, P.S., Venkateswarlu, D., Rayaprol, S., Ganesan, V., Boujelben, W., Kuberkar, D.G.: Magnetic and electrical studies on $\text{La}_{0.4}\text{Sm}_{0.1}\text{Ca}_{0.5}\text{MnO}_3$ charge ordered manganite. *J. Magn. Magn. Mater.* **381**, 470 (2015)
 42. Jia, R., Deng, D., He, P., Xu, Y., Feng, Z., Liu, Y., Cao, S., Zhang, J.: Crossover effect of inter-granular transport and quantum correction in Co-doping $\text{La}_{2/3}\text{Ca}_{1/3}\text{MnO}_3$ manganites. *J. Magn. Magn. Mater.* **329**, 65 (2013)
 43. Munirathinam, B., Krishnaiah, M., Devarajan, U., Esakki Muthu, S., Arumugan, S.: Synthesis, structural, electrical and Magnetic studies of $\text{La}_{0.5}\text{Ca}_{0.45-x}\text{Sr}_x\text{Ba}_{0.05}\text{MnO}_3$. *J. Phys. Chem. Solids* **73**, 925 (2012)
 44. Narjis, A., Elkaouachi, A., Biskupski, G., Daoudi, E., Limouny, L., Dlimi, S., Errai, M., Sybous, A.: Low temperature electrical resistivity of polycrystalline $\text{La}_{0.67}\text{Sr}_{0.33}\text{MnO}_3$ thin films. *Mater. Sci. Semicon. Proc.* **16**, 1257 (2013)
 45. Krichene, A., Solanki, P.S., Rayaprol, S., Ganesan, V., Boujelben, W., Kuberkar, D.G.: B-site bismuth doping effect on structural, magnetic and magnetotransport properties of $\text{La}_{0.5}\text{Ca}_{0.5}\text{Mn}_{1-x}\text{Bi}_x\text{O}_3$. *Ceram. Int.* **41**, 2637 (2015)
 46. Kondo, J.: Resistance minimum in dilute magnetic alloys. *Prog. Theor. Phys.* **32**, 37 (1964)